

## Probability distribution of the conductance in anisotropic systems

Marc Rühländer,<sup>1</sup> Peter Markoš,<sup>1,2</sup> and C. M. Soukoulis<sup>1</sup>

<sup>1</sup>*Ames Laboratory and Department of Physics and Astronomy, Iowa State University, Ames, Iowa 50012*

<sup>2</sup>*Institute of Physics, Slovak Academy of Sciences, Dúbravská cesta 9, 842 28 Bratislava, Slovakia*

(Received 28 March 2001; published 26 October 2001)

We investigate the probability distribution  $p(g)$  of the conductance  $g$  in anisotropic two-dimensional systems. The scaling procedure applicable to mapping the conductance distributions of localized anisotropic systems to the corresponding isotropic one can be extended to systems at the critical point of the metal-to-insulator transition. Instead of the squares used for isotropic systems, one should use rectangles for the anisotropic ones. At the critical point, the ratio of the side lengths must be equal to the square root of the ratio of the critical values of the quasi-one-dimensional scaling functions. For localized systems, the ratio of the side lengths must be equal to the ratio of the localization lengths.

DOI: 10.1103/PhysRevB.64.193103

PACS number(s): 71.30.+h, 71.55.Jv

The presence of disorder<sup>1</sup> may allow a system to make a transition from metallic to insulating behavior by varying the Fermi energy in an energy range where both extended and localized states are found, separated by a mobility edge. Characterizing this transition, one can employ transport properties, such as the conductance, or properties of the system's eigenstates, such as the correlation length for extended, metallic states or the localization length  $\xi$  for insulating states. At the mobility edge, a determination of the complete probability distribution  $p(g)$  of the conductance  $g$  (in units of  $e^2/h$ ) is needed. The critical point of the transition from metallic states to Anderson localized ones<sup>2</sup> is of particular interest. The distributions are well known to be normal and log-normal off the mobility edge towards the extended and the localized regime, respectively, whereas the exact form of the critical distribution is still under investigation.<sup>3–10</sup> For example, contrary to expectations, the critical distribution seems to vary even within the same universality class, depending on the boundary conditions perpendicular to the direction in which transport occurs.<sup>3–5</sup> Also, questions about the exact form of the large- $g$  tail ( $g > 1$ ) remain unanswered. Where calculations in  $2 + \varepsilon$  dimensions<sup>6</sup> indicate higher cumulants to diverge with system size, leading to a power law tail, numerical calculations<sup>7</sup> in three dimensions and analytical results for quasi-one-dimensional wires<sup>5</sup> show an exponential decay.

Anisotropic systems have recently been the focus of particular attention.<sup>11–16</sup> It is generally accepted that anisotropy does not change the universality class and that isotropic results can be recovered by performing a proper scaling of the anisotropic results. For anisotropic systems in a localized state, it is reasonable to assume that scaling the dimensions of the system by the corresponding localization lengths will make the system effectively isotropic. This procedure has been applied successfully<sup>11</sup> to the scaling function  $\Lambda = \lambda_M/M$ , which is a function of  $\xi/M$ , where  $\lambda_M$  denotes the finite size localization length of a quasi-one-dimensional strip of finite width  $M$  and  $\lambda_M \rightarrow \xi$  as  $M \rightarrow \infty$ . It was also shown<sup>17</sup> that the same scaling procedure works for the probability distribution in such a system.

In order to test the approach for critical states one must either face the numerical challenge of large three-

dimensional systems or take into account additional interactions (beyond the disorder potential) such as spin-orbit coupling.<sup>18</sup> Another possibility is the introduction of external magnetic fields as, e.g., in integer quantum Hall systems<sup>19</sup> or tight-binding models with random magnetic flux.<sup>20</sup> However, as a result of Anderson localization, extended states do not exist in two-dimensional systems of noninteracting electrons in a magnetic field, except at a singular energy near the center of each of the Landau subbands. At these critical energies  $E_c$  the localization length  $\xi$  diverges with a critical exponent  $\nu$ :  $\xi \propto |E - E_c|^{-\nu}$ .

Because significant finite size effects have to be expected, we decided to concentrate our research on two-dimensional systems, although the exact form of the critical distribution of the conductance depends on the dimensionality of the system.<sup>7</sup> The investigation of the self-averaging quantity  $\xi$  in integer quantum Hall systems yielded very encouraging results,<sup>15</sup> supporting the expectation that quantities of anisotropic systems can indeed be mapped to isotropic values by a simple rescaling scheme.

In this paper, we show a method of mapping the probability distributions of the conductance of anisotropic two-dimensional systems with a magnetic field perpendicular to the plane or with spin-orbit coupling to the probability distribution of the conductance for the corresponding isotropic system at the critical point, using a tight-binding model. It turns out that the ratio of the squares of the side lengths  $L_x$ ,  $L_y$  of the anisotropic system should be chosen equal to the ratio of the critical values  $\Lambda_x^c$ ,  $\Lambda_y^c$  of the quasi-one-dimensional scaling functions:

$$\frac{L_x^2}{L_y^2} = \frac{\Lambda_x^c}{\Lambda_y^c}. \quad (1)$$

In the following, we first describe the models and the numerical method we employed. Then we present and discuss our numerical results and finally summarize the conclusions of this work.

The tight-binding model uses the Hamiltonian

$$\mathcal{H} = \sum_{n,\tau} |n\tau\rangle \varepsilon_n \langle n\tau| + \sum_{n,\tau,n',\tau'} |n\tau\rangle V_{n,n'} \langle n'\tau'|, \quad (2)$$

where  $n, n'$  denotes the lattice site. Without spin-orbit interaction the “variables”  $\tau, \tau'$  take on only one value and the hopping integrals  $V_{n,n'}$  are scalar, otherwise they are  $2 \times 2$  matrices and the spin variables take on the values 1 or  $-1$ . In either case the site energies  $\varepsilon_n$  are independent of  $\tau$  and we take into account interactions only between neighboring lattice sites.

An external magnetic field enters the Hamiltonian via its vector potential  $\mathbf{A}$  ( $\nabla \times \mathbf{A} = \mathbf{B}$ ), which appears in the phases of the hopping integrals:

$$V_{n,n'} = t_{n,n'}^0 \exp\left(-2\pi i (e/h) \int_{\mathbf{r}_n}^{\mathbf{r}_{n'}} \mathbf{A}(\mathbf{r}) d\mathbf{r}\right). \quad (3)$$

The integral connects the lattice sites  $n$  (at  $\mathbf{r}_n$ ) and  $n'$  (at  $\mathbf{r}_{n'}$ ) in a straight line. For the systems under consideration, where the magnetic induction  $\mathbf{B}$  is perpendicular to the plane of the two-dimensional lattice, the gauge for the vector potential can be chosen such that the phases vanish in the direction perpendicular to  $\mathbf{A}$  and are integer multiples of some number  $2\pi\alpha$  in the direction parallel to  $\mathbf{A}$ . The value of the parameter  $\alpha$  then completely characterizes the influences of the magnetic field on the system. For rational  $\alpha$ , the denominator determines the number of bands in the density of states of the system without disorder.

The Evangelou–Ziman model<sup>21</sup> incorporates spin-orbit coupling by using the following hopping integrals:

$$V_{n,n'}^{\tau,\tau'} = t_{n,n'}^0 \left[ \delta_{\tau,\tau'} + \mu i \sum_{\nu} \sigma_{\tau,\tau'}^{\nu} t_{n,n'}^{\nu} \right], \quad (4)$$

where  $\nu = x, y, z$ , and  $\sigma^{\nu}$  are the Pauli matrices. The parameter  $\mu$  characterizes the strength of the spin-orbit interaction.

Both systems may be made anisotropic by choosing the value of  $t^0$  to be different in the two directions within the plane. Otherwise this parameter is a constant, independent of lattice site  $n$ . We bring disorder to the system by choosing all the site energies independently from a rectangular distribution of width  $W$  centered at 0, so that  $W$  is a measure of the strength of the disorder. The parameters  $t^{\nu}$  are also randomly selected from a uniform distribution on  $[-1/2, 1/2]$ . The energy scale is set by the larger of the two values for  $t^0$ , which is taken to be unity.

We calculate the conductance from the Landauer formula<sup>22</sup>

$$g = \text{Tr}(t^{\dagger} t) \quad (5)$$

where  $t$  is the transmission matrix. We suppose two semi-infinite leads are attached to opposite sides of the sample. Then  $t$  determines the transmission of an electron through the sample. The numerical procedure is based on the algorithms published by Ando<sup>23</sup> and by Pendry *et al.*<sup>23</sup>

The critical conductance distributions we calculated for isotropic quantum Hall systems at different disorder strengths show that finite-size effects become stronger the weaker the disorder. Where systems with  $W=4.0$  and  $W=2.0$  show a basically size-independent critical distribution of the conductance for squares of  $64 \times 64$  lattice sites, at  $W=0.5$  finite-size effects are still somewhat noticeable up to

systems with  $192 \times 192$  lattice sites. The anisotropic quantum Hall systems we investigated are characterized by  $\alpha = \frac{1}{8}$ . The anisotropies we chose were  $t_x^0/t_y^0 = 0.5$  at  $W=0.5$  and  $t_x^0/t_y^0 = 0.8$  at  $W=0.1$ . The latter was chosen mainly because we already had the data for the quasi-one-dimensional scaling function. As the disorder is even weaker than in the first case, finite-size effects are even stronger, and even at  $240 \times 240$  lattice sites the conductance distribution is far from the one we expect from our calculations of isotropic systems. Therefore, we will not be able to show that our procedure maps the two anisotropic conductance distributions to the critical distribution of isotropic systems for this extreme case. We will, however, be able to prove the somewhat weaker claim that our method transforms the two anisotropic distributions so that both have the same shape. In a square system, one expects that the distribution in the difficult hopping direction shows a more localized character than the one in the easy hopping direction. In an isotropic system, the distribution obviously cannot depend on the direction of transport. By making the system rectangular rather than square, i.e., shorter in the difficult hopping direction, it should be possible to obtain distributions in the two directions that are the same, thus making the anisotropic system effectively behave isotropically.

The task now is “How do we choose the correct ratio of side lengths of the rectangle?” From the research on localized systems<sup>11,17</sup> we know that in those cases, the ratio should be equal to the ratio of the localization lengths:

$$\left( \frac{L_x}{\xi_x} = \frac{L_y}{\xi_y} \Rightarrow \right) \frac{L_x}{L_y} = \frac{\xi_x}{\xi_y} \quad (6)$$

for localized systems, as these are obviously the appropriate length scales in their respective directions. This is of no use for critical systems as both localization lengths diverge at the transition. A closely corresponding *nondiverging* quantity is, however, available in the scaling function  $\Lambda_M = \lambda_M/M$ , which has a finite critical value, independent of the system width  $M$ . The finite-size localization lengths  $\lambda_{M,x}$  and  $\lambda_{M,y}$  have  $\xi_x$  and  $\xi_y$ , respectively, as their large- $M$  limits, and for large enough systems we can approximate Eq. (6) by

$$\frac{L_x}{L_y} = \frac{\lambda_{M,x}}{\lambda_{M,y}} \quad (7)$$

for localized systems at “large enough”  $M$ . The meaning of  $M$  in this context would be that of the system width perpendicular to the direction in which the localization length is measured, i.e.,  $M = L_y$  in  $\lambda_{M,x}$  and  $M = L_x$  in  $\lambda_{M,y}$ . Now, by multiplying both sides of Eq. (7) by  $L_x/L_y$  we have

$$\frac{L_x^2}{L_y^2} = \frac{L_x}{\lambda_{M,y}} \frac{\lambda_{M,x}}{L_y} = \frac{\Lambda_{M,x}}{\Lambda_{M,y}} \quad (8)$$

for large localized systems. Now  $\Lambda_M$  is a continuous function of  $E$  and for large enough systems at  $E_c$  should have reached its critical value. Therefore, we arrive at the conclusion that

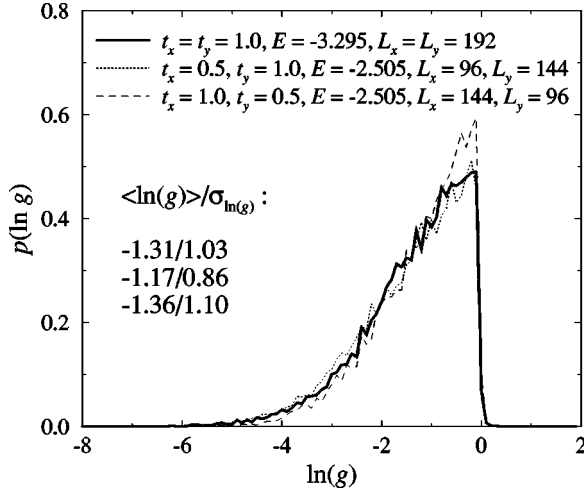


FIG. 1. The conductance distributions of an anisotropic rectangular system with a ratio of side lengths chosen according to Eq. (9). For comparison the corresponding distribution of an isotropic system is shown as well.

$$\frac{L_x}{L_y} = \sqrt{\frac{\Lambda_x^c}{\Lambda_y^c}} \quad (9)$$

should be the correct ratio for critical systems in order to make them behave like isotropic ones. Noting the relationship<sup>9,13,17</sup>

$$\sqrt{\Lambda_x^c \Lambda_y^c} = \Lambda_{\text{iso}}^c \quad (10)$$

we can write Eq. (9) in the alternate form

$$\frac{L_x}{L_y} = \frac{\Lambda_x^c}{\Lambda_{\text{iso}}^c} = \frac{\Lambda_{\text{iso}}^c}{\Lambda_y^c}. \quad (11)$$

We tested this prediction on the system with  $t_x^0/t_y^0=0.5$  and  $W=0.5$ , where the ratio  $\sqrt{\Lambda_x^c/\Lambda_y^c}$  is roughly 1.5. The result is shown in Fig. 1 together with the critical distribution for the isotropic system. The agreement is very good. For the other system with  $t_x^0/t_y^0=0.8$  and  $W=0.8$ , we have to deal with stronger finite-size effects and cannot expect to approach the form of the critical distribution we see in Fig. 1 for reasonable system sizes. Instead we merely show in Fig. 2 how the critical distributions change with the ratio of side lengths. The best value for the ratio according to Eq. (9) would be roughly 1.23. Figure 2 shows results for ratios of 1.0, 1.25, and 1.5. The averages of  $\ln(g)$  for the easy hopping direction decrease with increasing ratio from  $-4.09$  for the square to  $-4.40$  and  $-5.30$ , while the averages for the difficult hopping direction increase from  $-4.94$  for the square to  $-4.18$  and  $-4.03$ . Similarly, the standard deviations increase for the easy hopping direction from 1.90 for the square to 2.07 and 2.30, while they decrease for the difficult hopping direction from 2.24 for the square to 2.01 and 1.91. The values for a ratio of 1.25 are not equal but reasonably close, so that for larger systems, where a ratio of 1.23 might be practicable, we expect a better agreement of the two probability distributions.

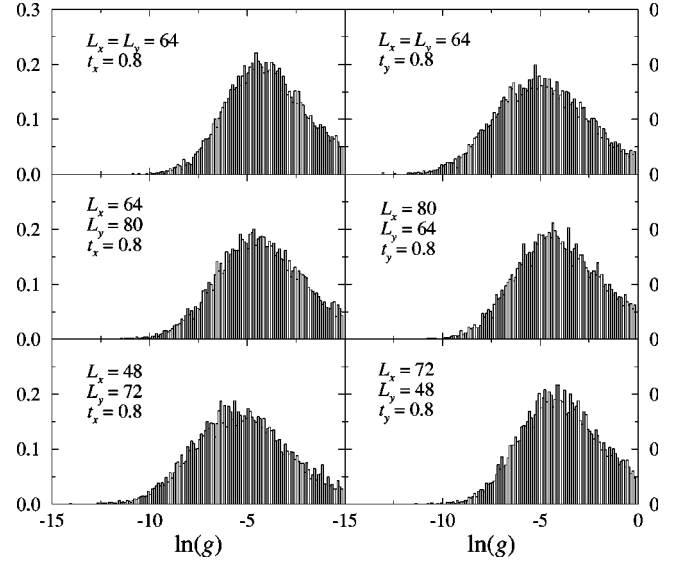


FIG. 2. Conductance distributions of an anisotropic system for varying ratios of the side lengths. The left panels refer to transport in the easy hopping direction, the right panels to transport in the difficult hopping direction. The ratio of side lengths is 1.0 for the top row, 1.25 for the middle row, and 1.5 for the bottom row.

Taking the best-ratio rectangle as the “undeformed” base, we can also see from Fig. 2 that similar “deformations” have similar effects in the two directions, that is, reducing the ratio by a factor  $\gamma$  in one direction will cause the ensemble average  $\langle \ln(g) \rangle$  in that direction to increase, and the standard deviation to decrease, while the trend is opposite in the perpendicular direction. However, reducing the ratio by the same factor  $\gamma$  in the other direction will result roughly in the same distributions as before, but with the one associated with the easy direction before now assigned to the difficult direction and *vice versa*.

That the same procedure also works for systems with spin-orbit coupling is shown in Fig. 3, where we plot the conductance distribution for an isotropic system with  $\mu = 1.0$  at  $E=0.1$  and  $W_c=6.7$  together with that of two an-

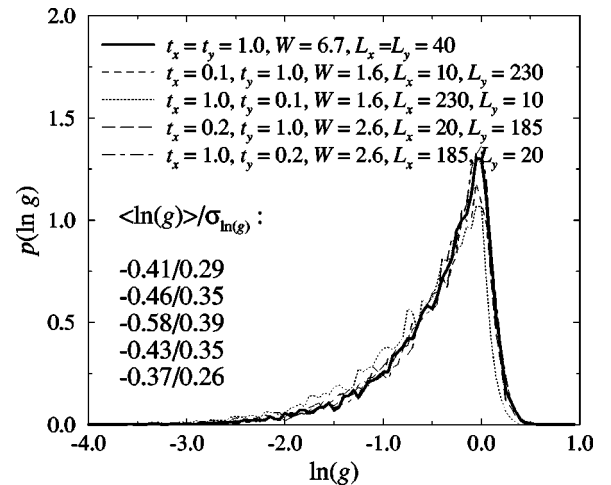


FIG. 3. The conductance distributions for an isotropic and two anisotropic systems with spin-orbit coupling.

isotropic systems, one with  $\mu=1.0$  and  $t_x^0/t_y^0=0.1$  at  $E=0.1$  and  $W_c=1.6$ , the other with  $\mu=1.0$  and  $t_x^0/t_y^0=0.2$  at  $E=0.1$  and  $W_c=2.6$ . The ratio of sidelengths, according to Eq. (9), should be 23.0 for the latter. We chose  $40\times 40$  lattice sites for the isotropic system,  $10\times 230$  lattice sites for the strongly anisotropic one, and  $20\times 185$  lattice sites for the anisotropic system with the weaker anisotropy. Again the agreement is very good.

We have shown that the scaling procedure applicable to mapping the conductance distributions of localized anisotropic systems to the corresponding isotropic one can be extended in a straightforward manner to systems at the critical point of the Anderson localization-delocalization transition

in both unitary and symplectic two-dimensional systems. Instead of the squares used for isotropic systems, one should use rectangles for the anisotropic ones, with a ratio of side lengths equal to the square root of the ratio of the critical values of the quasi-one-dimensional scaling function.

Ames Laboratory is operated for the U.S. Department of Energy by Iowa State University under Contract No. W-7405-Eng-82. This work was supported by the Director for Energy Research, Office of Basic Science. P.M. would like to thank IITAP and Ames Laboratory at Iowa State University for their hospitality and support and the Slovak Grant Agency for financial support.

- 
- <sup>1</sup>C. M. Soukoulis and E. N. Economou, *Waves Random Media* **9**, 255 (1999) and references therein.
- <sup>2</sup>For a recent review, see B. Kramer and A. MacKinnon, *Rep. Prog. Phys.* **56**, 1469 (1993).
- <sup>3</sup>K. Slevin and T. Ohtsuki, *Phys. Rev. Lett.* **78**, 4083 (1997); K. Slevin, T. Ohtsuki, and T. Kawarabayashi, *Phys. Rev. Lett.* **84**, 3915 (2000); K. Slevin and T. Ohtsuki, *Phys. Rev. B* **63**, 045108 (2001).
- <sup>4</sup>C. M. Soukoulis, X. Wang, Q. Li, and M. M. Sigalas, *Phys. Rev. Lett.* **82**, 668 (1999).
- <sup>5</sup>D. Braun, E. Hofstetter, G. Montambaux, and A. MacKinnon, *cond-mat/0101122* (unpublished).
- <sup>6</sup>B. Shapiro, *Phys. Rev. Lett.* **65**, 1510 (1990); A. Cohen, Y. Roth, and B. Shapiro, *Phys. Rev. B* **38**, 12 125 (1988); B. Shapiro, *Philos. Mag. B* **56**, 1031 (1987).
- <sup>7</sup>P. Markoš, *Phys. Rev. Lett.* **83**, 588 (1999).
- <sup>8</sup>K. A. Muttalib and P. Wölfle, *Phys. Rev. Lett.* **83**, 3013 (1999).
- <sup>9</sup>X. Wang, Q. Li, and C.M. Soukoulis, *Phys. Rev. B* **58**, 3576 (1998).
- <sup>10</sup>V. Plerou and Z. Wang, *Phys. Rev. B* **58**, 1967 (1998).
- <sup>11</sup>Qiming Li, S. Katsoprinakis, E. N. Economou, and C. M. Soukoulis, *Phys. Rev. B* **56**, R4297 (1997), and references therein.
- <sup>12</sup>F. Milde, R. A. Römer, and M. Schreiber, *Phys. Rev. B* **55**, 9463 (1997).
- <sup>13</sup>I. Zambetaki, Q. Li, E. N. Economou, and C. M. Soukoulis, *Phys. Rev. Lett.* **76**, 3614 (1996); I. Zambetaki, Q. Li, E. N. Economou, and C. M. Soukoulis, *Phys. Rev. B* **56**, 12 221 (1997).
- <sup>14</sup>N. Dupuis, *Phys. Rev. B* **56**, 9377 (1997); C. Mauz, A. Rosch, and P. Wölfle, *ibid.* **56**, 10 953 (1997).
- <sup>15</sup>M. Rühländer and C. M. Soukoulis, *Phys. Rev. B* **63**, 085103 (2001).
- <sup>16</sup>S. N. Evangelou, Sh. Xiong, P. Markoš, and D. E. Katsanos, *Phys. Rev. B* **63**, 144526 (2001).
- <sup>17</sup>X. Wang, Ph. D. thesis at Iowa State University; X. Wang, Q. Li, and C. M. Soukoulis, *Physica B* **296**, 280 (2001).
- <sup>18</sup>S. Hikami, *Prog. Theor. Phys.* **63**, 707 (1980).
- <sup>19</sup>For a review, see B. Huckestein, *Rev. Mod. Phys.* **67**, 357 (1995).
- <sup>20</sup>A. Furusaki, *Phys. Rev. Lett.* **82**, 604 (1999).
- <sup>21</sup>S. N. Evangelou and T. Ziman, *J. Phys. C* **20**, L235 (1987).
- <sup>22</sup>R. Landauer, *IBM J. Res. Dev.* **1**, 223 (1957); E. N. Economou and C. M. Soukoulis, *Phys. Rev. Lett.* **46**, 618 (1981); D. S. Fischer and P. A. Lee, *Phys. Rev. B* **23**, 6851 (1981).
- <sup>23</sup>T. Ando, *Phys. Rev. B* **44**, 8017 (1991); J. B. Pendry, A. MacKinnon, and P. J. Roberts, *Proc. R. Soc. London, Ser. A* **437**, 67 (1992).